# Triblock Copolymers in a Selective Solvent. 1. Aggregation Process in Dilute Solution

**E. Raspaud, D. Lairez,* and M. Adam**

*Laboratoire Léon Brillouin, CEA-CNRS, CE-Saclay, 91191 Gif-sur-Yvette Cedex, France*

**J.-P. Carton**

*Service de Physique de l'Etat Condensé, CE-Saclay, 91191 Gif-sur-Yvette Cedex, France*

*Received December 3, 1993; Revised Manuscript Received March 17, 1994®*

ABSTRACT: Triblock copolymers polystyrene–polyisoprene–polystyrene were studied in dilute solution in a selective solvent, i.e., a nonsolvent for polystyrene and a good solvent for polyisoprene. At a concentration equal to $1.6 \times 10^{-3}$ g/cm$^3$ triblock aggregates appear. Elastic and quasi-elastic light scattering experiments, as well as intrinsic viscosity measurements, performed on these solutions show a loose structure rather than a micellar structure for the aggregates. These experimental results are also discussed from a theoretical point of view.

## 1. Introduction

Polymer aggregation processes leading to multifarious and complex structures are an extensive research domain attracting a great deal of scientists. Starting from polymer properties which are now well-known in many aspects, a physicist can try one's hand at understanding the behavior of these aggregates. Varying the driving force of the aggregation, the number of possibilities seems to be unlimited as for a building set. A quick look at the literature concerning surfactant, zwitterion polymers, and block copolymers is enough to be convinced.

A tremendous effort is devoted to block copolymers in solution. One studies, for example, diblocks which are made of a succession of $N_A$ monomers A followed by $N_B$ monomers B, with A and B having different chemical nature and thus being incompatible. Depending on $N_A$, $N_B$, and the solvent quality for each block, several structures and long-range organizations are predicted theoretically and observed experimentally. For example, diblock copolymers A–B with $N_B > N_A$ diluted in a selective solvent, i.e., a good solvent for one block (B) and a nonsolvent for the other (A), are known to form micelles made of a core containing A blocks and a corona containing B blocks which adopt a starlike blob structure. In the case of selective solvent, an unsolved problem is the influence of the polymer topology on the aggregate conformation. For example, one may wonder whether diblock A–B and triblock A–B–B–A have the same behavior or not. In this paper, we report an experimental study of triblock aggregates obtained in a nonsolvent of the terminal blocks. While "flower"-like micelles are usually reported on the literature, our results obtained on one particular sample lead to another picture of the aggregate structure. These experimental results will also be discussed from a theoretical point of view.

## 2. Sample Characteristics and Experimental Conditions

The triblock copolymer polystyrene–polyisoprene–polystyrene studied in this paper was kindly provided by DEXCO. Its polydispersity index was given to be less than 1.02, and the weight ratios of each block are 15.3%, 69.4%, and 15.3%, respectively. This polymer sample was first characterized in dilute solution in a good solvent of the three blocks (tetrahydrofuran), by viscosimetry and static and dynamic light scattering experiments. The total weight-average molecular weight ($M_w$), the radius of gyration ($R_g$), the diffusion coefficient ($D$), and the intrinsic viscosity ($[\eta]$) were determined. Results are summarized in Table 1.

This paper is concerned with the aggregation process of this triblock copolymer in dilute solution in a selective solvent. Here, *n*-heptane was chosen, which is a nonsolvent for polystyrene terminal blocks and a good solvent for polyisoprene in the temperature range we worked with (above 40 °C).

Experimental results reported in this paper were obtained mainly by light scattering experiments. The polarized light source was either a $Ar^+$ (wavelength $\lambda_0 = 488$ nm) or a He–Ne laser ($\lambda_0 = 633$ nm), allowing an observation length scale comprised of between 27 and 270 nm. Dynamic light scattering experiments were performed using the self-beat technique, the time-averaged autocorrelation function of the scattered intensity being obtained using a Malvern 7032 multicorrelator. The small-angle neutron scattering experiment was performed on the PACE spectrometer in Saclay, and the observation length scale was comprised of between 2 and 34 nm. Viscosity measurements were performed using an Ubbelohde capillary viscosimeter.

## 3. Experimental Procedures and Results

**3.1. Static Light Scattering.** For a dilute polymer solution, calling $I_m$ and $I_s$ the measured scattered intensity by polymer solution and by solvent alone, respectively, the relevant quantity is the excess Rayleigh ratio due to light scattered by polymers in the solvent: $I = (I_m - I_s)/I_s$. Classically, $I(q)$ has the following form:

$$I(q) = (K/R_s)CM_wS(q)\,P(q) \qquad (1)$$

with $C$ the polymer concentration, $M_w$ the polymer weight-average molecular mass, $R_s$ the solvent Rayleigh ratio, $K = 4\pi^2n^2(\partial n/\partial C)^2/(N_A\lambda_0^4)$, $N_A$ Avogadro's number, and $n$ the refractive index of the solution. The refractive index increment $(\partial n/\partial C)$ of the triblock copolymer was calculated following ref 1 and using for homopolymer solutions the following values: $(\partial n/\partial C)_{PI} = 0.138$ and $(\partial n/\partial C)_{PS} = 0.215$. The scattering vector $q = (4\pi n/\lambda_0)\sin(\theta/2)$ corresponds to the inverse of the observation length scale. In dilute solution the structure factor $S(q)$ and the form factor $P(q)$ reflect space correlation between monomers belonging to different polymers and belonging to the same polymer, respectively. In the limit $q \to 0$, the structure factor $S(q)$ reflects the macroscopic properties of the solution and is proportional to the osmotic compressibility $(\partial\pi/\partial C)^{-1}$,

® Abstract published in *Advance ACS Abstracts*, April 15, 1994.

0024-9297/94/2227-2956$04.50/0 

**Table 1. Sample Characteristics Determined in a Good Solvent Solution (Tetrahydrofuran)**

| | |
|---|---|
| $M_w$ (g/mol) | $(1.65 \pm 0.08) \times 10^5$ |
| $R_g$ (nm) | $28 \pm 2$ |
| $D$ (cm$^2$/s) | $(45.5 \pm 0.5) \times 10^{-8}$ |
| $R_H$ (nm) | $10.0 \pm 0.1$ |
| $[\eta]$ (cm$^3$/g) | $95 \pm 2$ |

which is expressed by a virial expansion. One has

$$S(q)_{q\to 0} = (1 + 2M_wA_2C + ...)^{-1} \quad (2)$$

for $M_wA_2C < 1$, where $A_2$ is the second virial coefficient.

If the length scale $q^{-1}$ is sufficiently large compared to the radius of gyration $R_g$ of the polymers, the form factor $P(q)$ obeys Guinier's law:

$$P(q) = 1 - q^2R_{app}^2/3 + ... \quad (3)$$

where $R_{app}$, the apparent radius of gyration, is linked to $R_g$ by a virial expansion. Using eqs 1–3, the expression of the scattered intensity $I(q)$ at $qR_g < 1$ may be rewritten as:

$$I(q) = (K/R_s)CM_{app}(1 - q^2R_{app}^2/3) \quad (4)$$

with

$$M_{app} = M_w(1 - 2M_wA_2C)$$

The apparent mass $M_{app}$ of polymers in solution at a concentration $C$ is given by extrapolation of the scattered intensity per monomer $I(q)/C$ to $q = 0$, while the apparent radius of gyration $R_{app}$ is obtained by a mean-square linear fit of the inverse of the scattered intensity vs $q^2$.

When the length scale $q^{-1}$ is smaller than the apparent radius $R_{app}$, the scattered intensity depends strongly on the length scale. The scattered intensity per monomer $I(q)/C$ is only due to local space correlation between monomers in a volume $q^{-3}$ and is proportional to the number of monomers in this volume. This $q$-dependence gives us a direct access to the fractal dimension $d_f$ of polymers. In this $q$ range, the form factor can be expressed as:

$$P(q) = (qR_{app})^{-d_f} \quad (5)$$

Using eqs 1 and 4, $I(q)$ at $qR_{app} > 1$ can be rewritten as:

$$I(q) = (K/R_s)CM_{app}(qR_{app})^{-d_f} \quad (6)$$

with

$$M_{app} \sim R_{app}^{d_f}$$

Figures 1 and 2 show the concentration dependence of $M_{app}$ and $R_{app}$ determined by light scattering experiments. Above a given concentration equal to $(1.6 \pm 0.2) \times 10^{-3}$ g/cm$^3$, these quantities increase strongly with the concentration. This behavior is interpreted as a signature of the aggregation process for triblock copolymers. This is why, in the following, we will denote this concentration value the critical aggregation concentration *c.a.c.* by analogy with micellization processes which occur at concentration higher than the *c.m.c.*

In the concentration range below the *c.a.c.*, linear dependencies of $M_{app}$ and $R_{app}$ with concentration are due to interactions between polymers in solution and could be expressed by a virial expansion as mentioned above. Nevertheless, the variation of scattered intensity within this concentration range is too small to allow an accurate

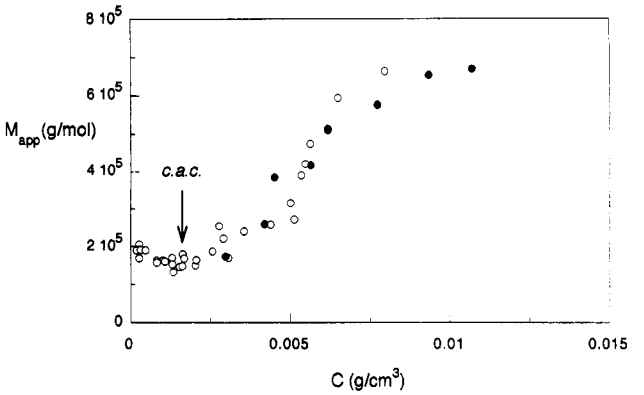


**Figure 1.** Concentration dependence at 50 °C of the apparent mass $M_{app} = I_0/(K/R_s)C$, where $I_0$ is the scattered intensity at $q = 0$. The apparent mass increases continuously above a given concentration denoted *c.a.c.*. Closed symbols correspond to the concentrations studied by quasi-elastic light scattering.

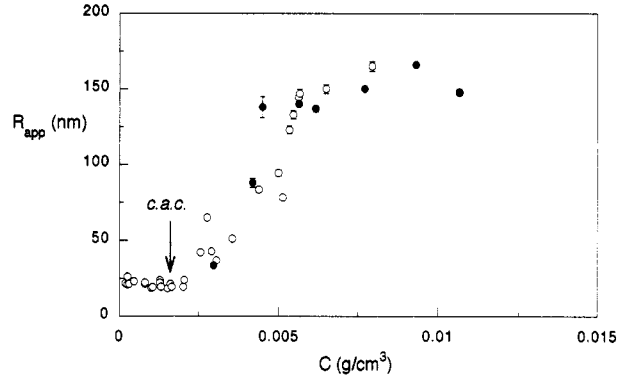


**Figure 2.** Concentration dependence at 50 °C of the apparent radius $R_{app}$. Above the *c.a.c.*, the radius increases strongly until a concentration on the order of $6 \times 10^{-3}$ g/cm$^3$, the value above which it remains constant. Closed symbols correspond to the concentrations studied by quasi-elastic light scattering.

determination of the second virial coefficient. Figures 1 and 2 only indicate a repulsive potential between polymers ($A_2 > 0$). Extrapolations of $M_{app}$ and $R_{app}$ to $C = 0$ lead to:

$$M_w = 1.68 \times 10^5 \text{ g/mol} \qquad R_g = 25 \pm 2 \text{ nm} \quad (7)$$

which is close to the values obtained for triblock copolymers in good solvent (see Table 1). Thus, the overlap concentration $C^* = M_w/(N_AR_g^3)$ of triblock copolymers can be estimated, and one finds

$$C^* = 1.7 \times 10^{-2} \text{ g/cm}^3 \quad (8)$$

In the concentration range above the *c.a.c.*, $R_{app}$ and $M_{app}$ increase strongly with the concentration until $C \cong 6 \times 10^{-3}$ g/cm$^3$, the value above which $R_{app}$ ramins constant while $M_{app}$ increases more slowly. In this concentration range two different behaviors of the scattered intensity $I(q)$ are observed:

(1) At $qR_{app} < 1$, $I(q)$ was fitted using eq 4 which allows us to determine $M_{app}$ and $R_{app}$. Their variations vs the total concentration are given in Figures 1 and 2. In this $q$-range, for the highest concentration, the measured mass (and radius of gyration) is larger by a factor 4 (8), than the expected value for isolated triblock copolymers. This indicates the presence of large triblock aggregates.

(2) At $qR_{app} > 1$, light scattering data can be fitted by Guinier's law (eq 4) with mass and radius on the order of those measured at concentrations below the *c.a.c.* This points out the presence of free isolated triblock copolymers still present in the solution.

In Figure 3, the inverse of the scattered intensity as a function of the square transfer vector measured for one sample is reported; it shows the method used to fit the low and high $q$ parts of the spectrum. These two behaviors of the scattered intensity spectra indicate clearly the presence of two scattering species in the solutions: aggregates and free copolymers which will be called unimers[2] in what follows. One has to note that, in such a case, it is not easy to separate the contribution of each scattering species. One can write

$$I(q) = I_{uni}(q) + I_{agg}(q) \tag{9}$$

The apparent radius measured at $qR_{app} < 1$, is a $z$-averaged quantity which follows the general expression:

$$R_{app} = \left[\frac{C_{uni}M_{uni}R_{uni}^2 + C_{agg}M_{agg}R_{agg}^2}{CM_{app}}\right]^{1/2} \tag{10}$$

assuming monodisperse aggregates, where $C$, $M$, and $R$ are concentration, mass, and radius of unimers and aggregates, respectively, depending on the subscript. It means that the apparent radius of gyration of aggregates is larger than the measured radius. More quantitative information concerning the aggregation process requires complementary data which were obtained using a quasi-elastic light scattering technique and are reported in the next section. We will see how these experiments allow us to deduce $C_{agg}M_{agg}/C_{uni}M_{uni}$; in all the cases the value of this ratio leads to an underestimation of the radius of the aggregates by less than 10%.

On one sample ($C = 4.7 \times 10^{-3}$ g/cm$^3$) diluted in deuterated $n$-heptane, a small-angle neutron scattering experiment was performed. For this sample, in order to see the scattered intensity spectrum in a wide $q$-range, light and neutron scattering data are plotted on the same figure (Figure 4) using arbitrary units (neutron scattering data being scaled by a numerical factor). This result will be discussed later on.

**3.2. Quasi-Elastic Light Scattering.** A quasi-elastic light scattering device allows the time-dependent fluctuations of the refractive index of a medium to be analyzed by computing the time-averaged autocorrelation function of the scattered intensity signal $I(q,t)$. In the Gaussian approximation[3] the relaxation function $g(q,t)$ of these fluctuations can be written as:

$$g(q,t) = \left[\frac{\langle I(q,0)\, I(q,t)\rangle - \langle I(q,t)\rangle^2}{\langle I(q,t)^2\rangle - \langle I(q,t)\rangle^2}\right]^{1/2} \tag{11}$$

Experimentally, fluctuations of the refractive index due to concentration fluctuations ($dn/dC$) are larger than those due to temperature fluctuations ($dn/dT$). Therefore, $g(q,t)$ reflects the translatory motion of the set of scattering units which scatter coherently. It may be, for example, the diffusive motion of polymers in dilute solution when they are observed at length scales $q^{-1}$ larger than their radius of gyration. In this case, the relaxation function $g(q,t)$ is the simple exponential decay having a characteristic time $\tau_c$ which is the time for the polymers to cover a distance $q^{-1}$. $D$ being the diffusion coefficient of the polymers, at $qR_g < 1$, one has

$$D = 1/\tau_c q^2 \tag{12}$$

In this $q$-range, the diffusion coefficient so measured is a constant independent of $q$, linked to the hydrodynamic radius $R_H$ of polymers through Stokes' law:

$$D = kT/6\pi\eta_s R_H \tag{13}$$

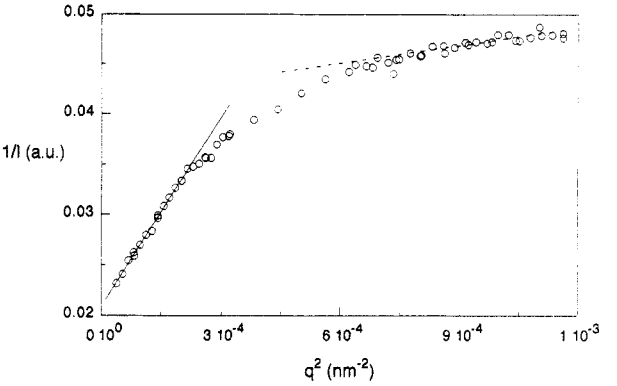


**Figure 3.** Guinier plot of the light scattered intensity measured on one sample having a concentration $C = 4.5 \times 10^{-3}$ g/cm$^3$. The inverse of the scattered intensity, $I$, as a function of the square of the transfer vector $q$ shows two linear behaviors in the low and high $q$-range, respectively. Straight lines correspond to mean-square linear fits of each part: the full line corresponds to $R_{app}$ = 94.6 nm; the dashed line corresponds to $R_{app}$ = 21 nm.

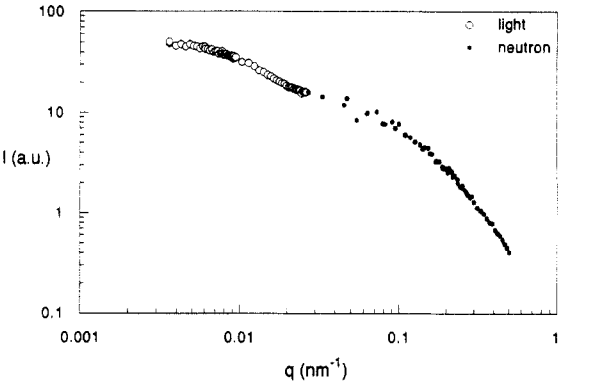


**Figure 4.** Light and neutron scattered intensity in arbitrary units (neutron data were multiplied by a given factor for juxtaposition) versus the transfer vector $q$, measured on one sample at $C = 4.7 \times 10^{-3}$ g/cm$^3$.

where $k$ is Boltzmann's constant, $T$ the temperature, and $\eta_s$ the solvent viscosity. At smaller length scales ($qR_g > 1$) measurements are sensitive to concentration fluctuations inside the polymer. In this case, the characteristic time depends strongly on hydrodynamical interactions between monomers of the same molecule. In the Zimm limit, valid, for example, in the case of linear polymers in dilute solutions, the measured characteristic time $\tau$ corresponds to the diffusive motion of parts of the molecule having a hydrodynamic radius equal to $q^{-1}$. This leads to $q^{-3}$ scaling of the time $\tau$ which characterizes internal modes of loose structure like linear or branched polymers in dilute solution.[4,5] In some other cases, for example, star polymers which behave like hard spheres,[6] small parts of molecules cannot diffuse irrespective of the others and the diffusion coefficient of the overall molecule is observed whatever the length scale $q^{-1}$.[7]

In the present study, $g(t,q)$ was measured below and above the *c.a.c.* and analyzed considering the static light scattering results reported in the previous section.

In the concentration range below the *c.a.c.*, the relaxation function $g(t,q)$ is found to be a simple exponential decay in the entire $q$-range. The diffusion coefficient $D_S = 1/(\tau_c q^2)$ is found to be independent of the scattering vector $q$ and of the concentration $C$ and is found to be equal to:

$$D_S = (7.3 \pm 0.3) \times 10^{-7}\ \text{cm}^2/\text{s} \tag{14}$$

leading to the hydrodynamic radius:

$$R_H = 10.8 \pm 0.5\ \text{nm} \tag{15}$$

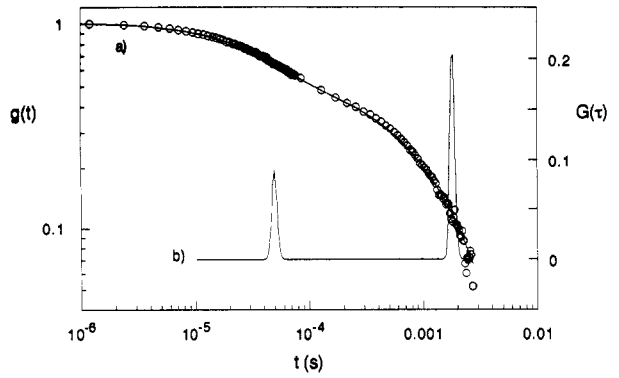


**Figure 5.** Log–log plot of the quasi-elastic light scattering relaxation function obtained on one sample at a given angle ($C = 1.07 \times 10^{-2}$ g/cm$^3$, $qR_{app} = 3$). The full line a corresponds to the best fit obtained by summation of one simple exponential and of one stretched exponential: $g(t) = 0.40 \exp(-t/40 \times 10^{-6}) + 0.60 \exp(-t/0.89 \times 10^{-3})^{2/3}$). The full line b results from a maximum entropy fit for the relaxation function.

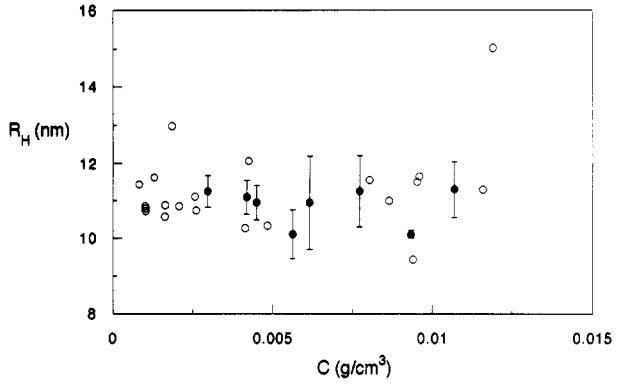


**Figure 6.** Hydrodynamic radius of unimers vs the total concentration, deduced from the short-time mode of the quasi-elastic light scattering relaxation function: $R_H = \tau_S q^2 kT/6\pi\eta_s$, where $\tau_S$ is the short characteristic time, $q$ the transfer vector, and $\eta_s$ the solvent viscosity. The so-measured radius is found to be in agreement with the one measured in good solvent solution ($R_H$ in THF, see Table 1) whatever the temperature (40, 50, and 60 °C) and the concentration. Closed symbols correspond to measurements performed at 50 °C.

This result is consistent with the diffusive motion of isolated triblock copolymers which are only present in the solution in this concentration range (see Table 1). The radius $R_g$ of triblock measured by static light scattering (eq 7) is sufficiently small that $qR_{app}$ is always smaller than 1. As for the independence of the diffusion coefficient on the concentration, it implies weak interactions between polymers.

In the concentration range above the *c.a.c.*, static light scattering results suggest two well-defined characteristic times for the relaxation function $g(t,q)$, corresponding to unimers and aggregates. In order to confirm this expectation, $g(t,q)$ was first analyzed using the maximum entropy method[9] which gives access to the relaxation time distribution function $G(\tau)$ defined by $g(t) = \int G(\tau)\, e^{-t/\tau}\, d\tau$. Figure 5 shows an example of the relaxation function measured on one sample at $C = 1.07 \times 10^{-2}$ g/cm$^3$ and $qR_{app} = 3$. Spectral analysis using the maximum entropy method indicates clearly the presence of two well-separated relaxation modes. The peak in the time distribution function corresponding to the fast mode is quite symmetric as expected for a simple exponential relaxation, while the slow mode shows a dissymmetry, as would be the case for a stretched exponential relaxation mode. Indeed, this relaxation function was obtained at length scale $q^{-1}$ intermediate between the radius of unimers and the one of aggregates. Therefore, one expects for the relaxation function (a) a short time corresponding to the diffusive mode of unimers and (b) a long time corresponding either to the internal motion or to the diffusion of the aggregates, depending on the hydrodynamic interactions taking place between monomers inside the aggregates.

One can show that, in the case of linear polymers, the $q^{-3}$ dependence of the characteristic times corresponding to internal modes comes with a stretched exponential relaxation function having an exponent $\beta = 2/3$.[5,8] In order to analyze the quasi-elastic light scattering data within this context, the relaxation function $g(t,q)$ was fitted by the method of cumulants applied to its short- and long-time parts. Subscripts S and L refer to short and long times, respectively. The following general form was used:

$$g(t,q) = A_S(q)\, e^{-t/\tau_S} + A_L(q)\, e^{-(t/\tau_L)^{\beta}} \qquad (16)$$

with $A_S(q) + A_L(q) = 1$ and $\beta = 1$ or $^2/_3$ according to the best fit. This procedure allows a rapid determination of the parameters $A_S$, $A_L$, $\tau_S$, and $\tau_L$ which have a direct physical meaning and is sufficiently accurate to describe the overall relaxation function as is shown on Figure 5.

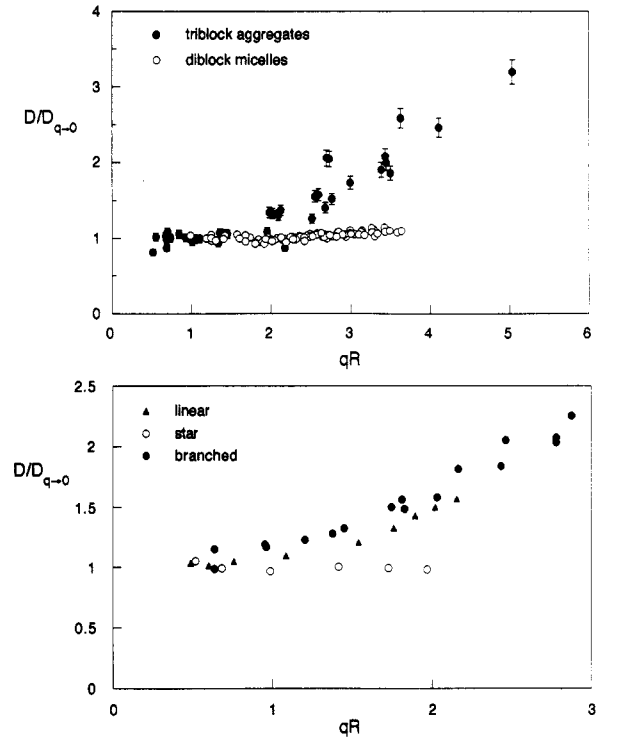


**Figure 7.** Reduced apparent diffusion coefficient $D/D_{q\to 0}$ vs $qR$. For triblock aggregates $R = R_{app}$ and $D = D_L = 1/\tau_L q^2$, where $\tau_L$ is the long characteristic time of the quasi-elastic light scattering relaxation function. (a) Comparison of triblock aggregates and diblock micelle behaviors.[23] (b) Comparison of linear,[5] branched,[22] and star polymer behaviors.[7] At $qR > 1$, triblock aggregates and linear and branched polymers show internal modes, while diblock micelles as well as star polymers show diffusive motion whatever $qR$.

Experimentally one obtains a diffusion coefficient $D_S = 1/\tau_S q^2$ independent of the scattering vector and of the concentration, which is equal to the diffusion coefficient measured below the *c.a.c.* This confirms the previous interpretation which assigned the short time to the diffusive motion of unimers. Figure 6 shows, at different temperatures, the independence of the hydrodynamic radius $R_H = kT/6\pi\eta_s D_S$ on the concentration.

Depending on the $q$-range, as shown in Figure 7a, one observes two behaviors for the diffusion coefficient $D_L = 1/\tau_L q^2$ assigned to the presence of aggregates:

(1) For $qR_{app} < 1$ the slow relaxation mode is a simple exponential ($\beta = 1$) and corresponds to a diffusive motion:

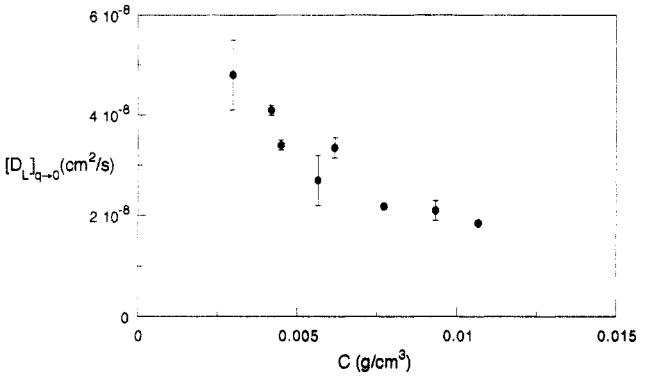


**Figure 8.** Concentration dependence of the diffusion coefficient of triblock aggregates.

the diffusion coefficient $D_L$ in this $q$-range is independent of $q$. Figure 8 shows that $[D_L]_{q\to 0}$ decreases with the concentration.

(2) For $qR_{app} > 1$, the best fit is obtained using a stretched exponential ($\beta = 2/3$) for the slowest relaxation mode. The measured diffusion coefficient $D_L$ scales as $q$ and reveals internal modes ($\tau_L \sim q^{-3}$). $D_L$ can be written as:

$$D_L \sim [D_L]_{q\to 0}(qR_{app}) \tag{17}$$

with

$$[D_L]_{q\to 0} \sim 1/R_{app}$$

Further information is contained in the $q$-dependence of the amplitude ratio $A_L/A_S$. The amplitudes of the two modes observed in the relaxation function reflect the contribution of each species to the total scattered intensity; one has the following equalities:

$$I(q) = I_{agg}(q) + I_{uni}(q) = I_0([A_L]_{q\to 0}P_{agg}(q) + [A_S]_{q\to 0}P_{uni}(q)) \tag{18}$$

$$A_L(q) = I_{agg}(q)/I(q) \quad \text{and} \quad A_S(q) = I_{uni}(q)/I(q) \tag{19}$$

where $I_0$, $P_{agg}(q)$, and $P_{uni}(q)$ are the total scattered intensity at $q = 0$ and the form factors of aggregates and unimers, respectively. In the whole experimental $q$-range, the length scale is sufficiently large compared to $R_{uni}$ to consider the contribution of unimers to the total scattered intensity as a $q$-independent constant: $P_{uni}(q) = 1$. This leads to:

$$\frac{A_L(q)}{A_S(q)} = \left[\frac{A_L}{A_S}\right]_{q\to 0} P_{agg}(q) \tag{20a}$$

$$\frac{I(q) - I_0[A_S]_{q\to 0}}{I_0[A_S]_{q\to 0}} = \left[\frac{A_L}{A_S}\right]_{q\to 0} P_{agg}(q) \tag{20b}$$

Consequently, it is possible to deduce the form factor $P_{agg}(q)$ of aggregates following two procedures: first from the variation of the ratio $A_L/A_S$ vs $q$ (eq 20a) and second from the analysis of the static light scattering spectra using eq 20b. Static and dynamic light scattering data are in good agreement (see Figure 9). Whatever the method, the temperature, and the concentration, a single curve for $P_{agg}(q)$ is found which shows a weak $q$-dependence for $qR_{app} < 1$ and a power law at $qR_{app} > 1$. One can write

$$P_{agg}(q) = f(qR_{app}) \tag{21}$$

with

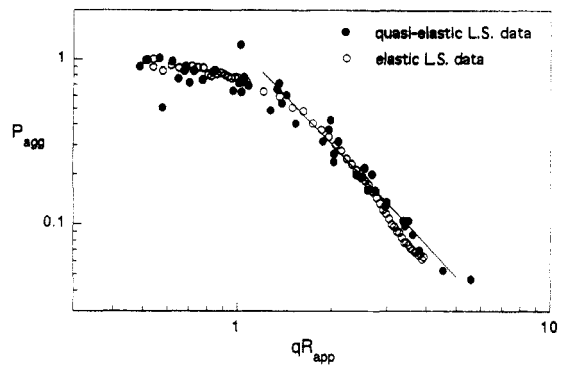


**Figure 9.** Form factor of aggregates, $P_{agg}$, as a function of the reduced quantity $qR_{app}$ obtained by static and quasi-elastic light scattering measurements. Quasi-elastic data obtained on different samples at different concentrations above the *c.a.c.* are superimposed, while static measurement corresponds to a sample at $C = 7.72 \times 10^{-3}$ g/cm$^3$. The straight line is a guide for the eyes having a slope −2.

$$f(qR_{app}<1) = 1 \quad \text{and} \quad f(qR_{app}>1) = (qR_{app})^{-d_f}$$

The fractal dimension is found to be $d_f = 2.0 \pm 0.2$. Figure 10 shows the increase of $[A_L/A_S]_{q\to 0}$ with the total concentration $C$, in agreement with the previous results reported in Figure 1. This concentration dependence and the total scattered intensity $I_0$ coming from static measurements can provide more information about the aggregation process. This will be discussed later on.

**3.3. Viscosimetry.** For a polymer solution, the quantity of interest is the specific viscosity, $\eta_{Sp}$, corresponding to the relative increase of the viscosity due to the presence of polymers:

$$\eta_{Sp} = \frac{\eta - \eta_s}{C\eta_s} = [\eta](1 + k_H[\eta]C) \tag{22}$$

where $\eta$ and $\eta_s$ are the solution and solvent viscosity, respectively, and $k_H$ is the Huggins constant. The quantity $[\eta]$ is called the intrinsic viscosity and has the dimension of the inverse of a concentration. In solution, hydrodynamic interactions are important; i.e., the polymer behavior corresponds to the Zimm limit. Furthermore, in zero shear flow, no deformation of the polymer occurs during the experiment. These two remarks allow us to apply the Einstein relation which links the viscosity $\eta$ to that of a solution of hard spheres occupying a volume fraction $\Phi$: $\eta = \eta_s(1 + {}^5/_2\Phi)$. From eq 22 it may be seen that $[\eta] \sim \Phi/C$ which is the inverse of the overlap concentration $C^*$ of polymers, i.e., their internal concentration ($\Phi \sim nR^3$ and $C \sim nM$ leading to $\Phi/C \sim R^3/M = 1/C^*$):

$$[\eta] \sim 1/C^* \tag{23}$$

Viscosity measurements were performed using a Ubbelohde capillary viscosimeter described elsewhere.[10] We found a similar concentration dependence of the reduced viscosity above and below the *c.a.c.* comparable to the one measured in good solvent solutions. By extrapolation to zero concentration, we have an intrinsic viscosity of triblock copolymers in *n*-heptane equal to $[\eta] = 67.0 \pm 0.5$ cm$^3$/g. Figure 11 shows the reduced specific viscosity $(\eta_{Sp} - [\eta])/[\eta]^2 = k_H C$ vs the concentration $C$ for triblock/*n*-heptane solutions and triblock/tetrahydrofuran solutions. No significant modification of the apparent Huggins coefficient is found, indicating clearly that unimers and aggregates have the same internal concentration $C^*$.

## 4. Discussion

**4.1. Experimental Results Interpretation.** The aggregation of block copolymers in a selective solvent is

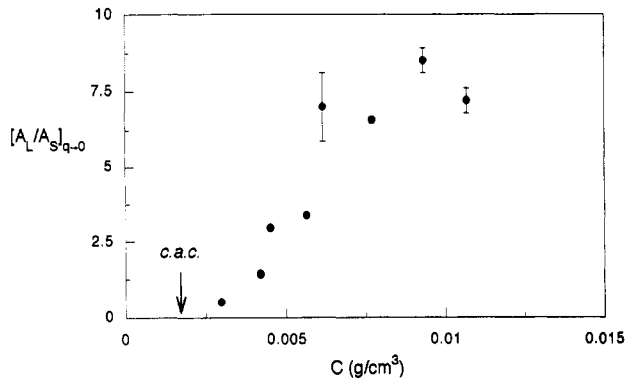


**Figure 10.** Concentration dependence of the $q = 0$ limit of amplitude ratio $(A_L/A_S)_{q\to 0}$ of the two quasi-elastic relaxation modes.

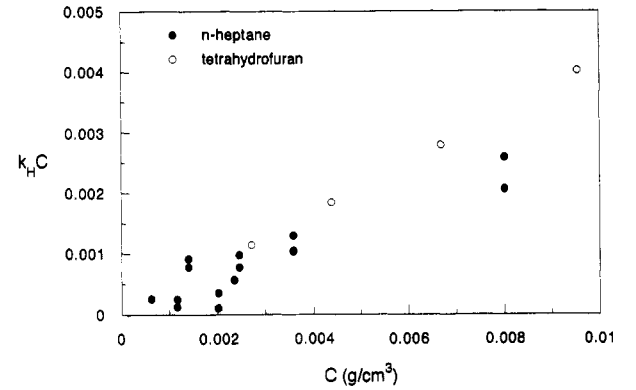


**Figure 11.** $(\eta_{Sp} - [\eta])/[\eta]^2 = k_HC$ (where $\eta_{Sp}$ is the specific viscosity and $[\eta]$ in intrinsic viscosity) as a function of the concentration in good solvent (tetrahydrofuran) and selective solvent (*n*-heptane). The concentration behavior is identical below and above the *c.a.c.* and comparable to the one observed in good solvent solution. This indicates that unimers and aggregates have the same overlap concentration $C^*$.

very often described as a micellization process leading to spherical starlike aggregates. For diblock copolymers, this description is encountered in both theoretical[11-13] and experimental[2,14,15] literature. In this picture, the driving force of the aggregation is the interfacial tension between the solvent and the polymer block which is in a nonsolvent situation. It leads to a very small critical micellar concentration (*c.m.c.*) and to a spherical conformation of the aggregates. It is often assumed that, from a theoretical point of view, there is no difference between diblock and triblock micellization. Triblock copolymers diluted in a nonsolvent of the terminal blocks are expected to form flower-like micelles, the loss of entropy which corresponds to the backfolding of the middle block being negligible compared to the enthalpic term.[16,17] These expectations are claimed to be verified in most of the cases.[17-19] There are obvious discrepancies between this common point of view and the results reported here. The first of them is the unusual high value of the critical concentration *c.a.c.* $= (1.6 \pm 0.2) \times 10^{-3}$ g/cm$^3$ which is larger than the value reported for diblock micellization.[2] Such a concentration value implies that there is a large amount of free unimers still present in the solution above the *c.a.c.* Due to them, the analysis of static scattering spectra is not easy. Nevertheless, the scattered intensity (see Figure 4) shows neither a $q^{-3}$ sharp decrease at $qR_g = 1$, which is characteristic of star-shaped polymers, nor a $q^{-4}$ Porod's behavior expected for structures having a sharp boundary as micelles with a high association number.[20,21] This result is confirmed by the form factor of triblock aggregates deduced from the analysis of both static and quasi-elastic light scattering data (see Figure 9). Moreover, examination of the dynamical behavior of the aggregates shows clearly

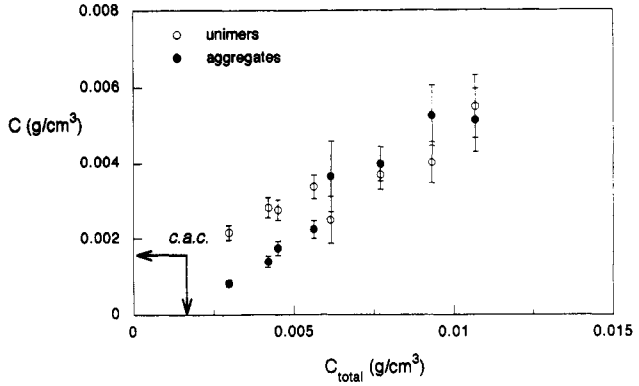


**Figure 12.** Variation of unimer and aggregate concentrations (in g/cm$^3$) versus the total concentration.

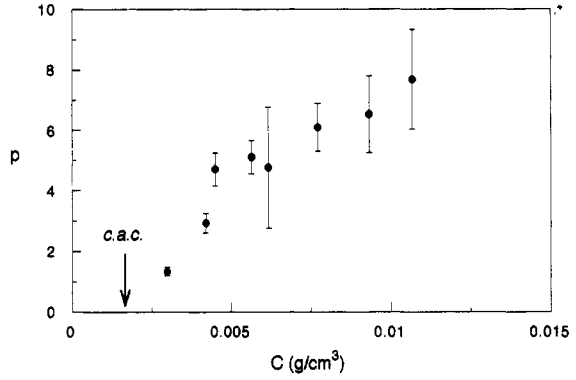


**Figure 13.** Variation of the aggregation number $p$ as a function of the total concentration.

internal modes ($D_L \sim q$) characteristic of loose structures as linear or branched polymers in the dilute regime, while compact or starlike micelles would lead to a diffusive mode whatever $qR_g$. Parts a and b of Figure 7 allow us to compare the $q$-dependence of the diffusion coefficient obtained for triblock aggregates, linear homopolymers,[5] and branched homopolymers[22] with the diffusive mode observed for stars[7] and diblock micelles whatever $qR_g$.[23]

From the concentration dependence of the total scattered intensity and of the amplitudes $A_L$ and $A_S$ of the two relaxation modes determined by quasi-elastic light scattering, one can obtain more details about the growth of aggregates. Neglecting interactions between unimers and/or aggregates and taking for the mass of unimers the apparent one measured at the *c.a.c.*, one gets the concentrations of unimvers and aggregates and the association number $p$ as a function of the total concentration:

$$C_{uni} = \frac{I_0[A_S]_{q\to 0}}{M_{uni}} \quad \text{and} \quad C_{agg} = C - C_{uni} \tag{24}$$

$$p = \frac{M_{agg}}{M_{uni}} = \left[\frac{A_L}{A_S}\right]_{q\to 0} \frac{C_{uni}}{C_{agg}} \tag{25}$$

Results are plotted on Figures 12 and 13. A continuous increase of $C_{uni}$, $C_{agg}$, and $p$ with the total concentration is found. Once again this result is in opposition to the classical micellization picture within which the degree of association $p$ and the concentration of unimers are expected to be independent of the concentration (the concentration of unimers is expected to be equal to the *c.m.c.*). Such a nonconstant unimer concentration would imply a polydisperse population of aggregates.

It is tempting to compare the concentration dependence of the association number $p$ to that of the apparent radius (Figures 13 and 2). It is readily seen that both quantities increase by a factor of 8, which seems to be inconsistent

with a fractal dimension, $d_f$, of order 2 (Figure 9). This result constitutes an additional argument in favor of the polydispersity of aggregates. The apparent radius and mass actually correspond to quantities averaged in different ways: the apparent mass is a weight-averaged quantity (ratio of the second moment to the first moment of the distribution), while the radius is a $z$-averaged quantity (ratio of the third to the second moment). Obviously, the latter is more sensitive to large aggregates than the former and thus would be overestimated in the case of a polydisperse population. However, the existence of a critical aggregation concentration and the presence of two well-defined modes in the quasi-elastic light scattering data suggest that there is a gap in the size distribution between the unimer and the smallest aggregate size. This topic will be discussed in the following section in relation with the possible structures for the aggregates.

Let us return to the viscosity measurements reported in section 3.3. These results indicate that the internal concentration $C^*$ remains unaffected by the aggregation process. Once more this would not be the case for triblock star micelles, for which the overlap concentration is expected to scale as $C^*_{star} \sim p^{2/5} C^*_{unimers}$.[21]

Thus viscosity and elastic and quasi-elastic light scattering results argue in favor of a loose aggregate structure remaining unimer conformation unaffected.

**4.2. Theoretical Point of View.** Our experimental results are understandable in terms of the theoretical work of ten Brinke and Hadziioannou[24] which outlines the difference between diblock and triblock aggregation. The authors do not expect triblocks to form micelles because of the loss of entropy due to the backfolding of the middle block. Indeed, branch-like triblock aggregates so-predicted were actually observed in recent computer simulations.[25] In this section simple theoretical considerations will show that, among the various possible structures one may imagine for the aggregate structure, flower-like micelles are unfavorable.

**4.2.1. Unimers and Critical Aggregation Concentration.** The simplest approach to critical aggregation assumes an equilibrium between free unimers and large aggregates. Equality between chemical potentials at the critical aggregation concentration $\phi_{c.a.c.}$ leads to:

$$\phi_{c.a.c.} = e^{(E_{agg}-E_1)/kT} \tag{26}$$

where $E_{agg}$ and $E_1$ are the free energy per chain for the aggregates and unimers, respectively. Expecting $E_{agg} \ll E_1$, due to the large size of the aggregates:

$$\phi_{c.a.c.} = e^{-E_1/kT} \tag{27}$$

Thus the critical aggregation concentration depends essentially on the unimer state, whatever type of aggregation occurs.

Free triblock copolymers ABA diluted in a nonsolvent of the terminal block can adopt two main different conformations: self-associated (ring shaped) or not (dumbbell shaped) (see Figure 14).[25] The interfacial energy between A blocks and the solvent is smaller in the former case than in the latter, but an entropy penalty is paid due to the backfolding of the middle B-block. This entropy loss is written in a phenomenological form following ten Brinke and Hadziioannou:[24]

$$F_{loop}/kT = \frac{3}{2}\beta \ln \tilde{N}_B \tag{28}$$

where $\tilde{N}_B$ is the number of statistical segments of the middle block, i.e., monomers for an ideally flexible polymer. The origin of the coefficient $\beta$ is worth discussing. In the case of end-to-end looping, one has $\beta = 1$ and $\beta = 1.3$ for Gaussian and excluded-volume chains, respectively. These values stems from the return probability $P_N(a)$ (see, for instance, ref 4, p 39). Calling $r$ the end-to-end distance, its distribution law has the general form:

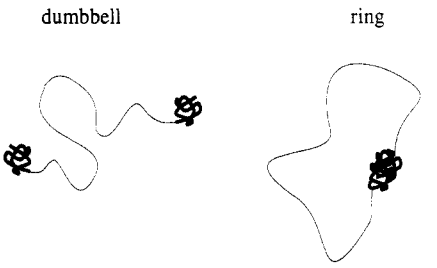


**Figure 14.** Dumbbell- and ring-shaped conformations of triblock copolymers in a selective solvent (nonsolvent of the terminal block).

$$P_N(r) \sim \frac{1}{R^3} f\left(\frac{r}{R}\right) \tag{29}$$

$R = aN^\nu$ being the radius of the polymer and $a$ the size of the statistical segment. One has $f(a/R) \sim (a/R)^{(\gamma-1)/\nu}$.[26] For triblock copolymers, more complicated effects can alter the value of $\beta$ when the degree of polymerization $N_A$ of the terminal blocks is increased.[25] One effect is due to the excluded volume due to the A core, which tends to repel the chain: it would increase the value of $\beta$ as the self-excluded volume does. On the contrary, when the radius of the core is not negligible compared to $R$, one has to take into account all possible locations of the second end point on the core surface. The extreme case corresponds to an infinite radius of the core; integrating eq 29 over a plane, one finds $\beta = 0.4$, not far from the value reported in ref 25 and probably the lower bound for $\beta$.

The triblock unimer conformation will result in a competition between the loss of entropy due to the backfolding of the middle block and the attraction between the terminal block due to interfacial energy. When

$$\frac{3}{2}\beta \ln \tilde{N}_B > (2 - 2^{2/3})\gamma a^2 (3(4\pi)^{1/2} N_A)^{2/3} \tag{30}$$

i.e., when $\tilde{N}_B$ is larger than one limit value $\tilde{N}^*_B$, dumbbell-shaped conformation has a lower energy. In this expression, $\gamma$ is an effective surface tension (in $kT$ unit) between the core and the solvent and $\beta$ depends on both $N_A$ and $N_B$. The limit value $\tilde{N}^*_B$ is naturally expressed using the solubility concentration, $\phi_s$, at the same temperature of a A homopolymer having the same degree of polymerization $N_A$ as the block copolymer. Approximately:

$$\ln\left(\frac{1}{\phi_s}\right) = \gamma a^2 (3(4\pi)^{1/2} N_A)^{2/3} \tag{31}$$

leading to:

$$\ln \tilde{N}^*_B = \frac{0.3}{\beta} \ln\left(\frac{1}{\phi_s}\right) \tag{32}$$

Let us return to the experiments reported in this paper. The triblock copolymer used has $N_A = N_{PS} = 200$ and $N_B = N_{PI} = 1500$. The solubility concentration in $n$-heptane of a $4 \times 10^4$ g/mol polystyrene ($N_{PS} = 400$) was measured by light scattering to be equal to $4 \times 10^{-5}$ g/g. This yields $\phi_s \cong 1.7 \times 10^{-3}$ g/g for $N_{PS} = 200$; using $\beta = 0.4$ (the most favorable value for ring-shaped conformation) one obtains

$$\tilde{N}_B^* \cong 100 \quad (33)$$

The condition $\tilde{N}_B > \tilde{N}_B^*$ is generally fulfilled, and most of the free unimers are expected to adopt a dumbbell conformation. This is experimentally confirmed by the radius of gyration of unimers in selective solvent (*n*-heptane) which is found comparable to the one measured in good solvent (THF), while ring-shaped polymers are expected to have a radius $\sqrt{2}$ smaller than linear polymers.[27] The energy $E_1$ of this reference state corresponds to twice the interfacial energy of one A block; it is found in our case ($N_A$ = 200) that

$$E_1 \cong 13\ kT \quad (34)$$

In this case, if large and strongly aggregated objects were to appear at $\phi_{c.a.c.}$ so that eq 27 would hold, one should have $\phi_{c.a.c.} = \phi_s^2 \cong 3 \times 10^{-6}$ g/g (while for diblock copolymers corresponding to half of a triblock, one should have $\phi_{c.a.c.} = \phi_s$). This is much too small compared with our experimental value $\phi_{c.a.c.} \cong 2.5 \times 10^{-3}$ g/g. Since $E_{agg}$ is not very small compared to $E_1$, it can be concluded that the aggregates are small or loose, or both. The experimental results reported here show that they are small and loose.

**4.2.2. On the Existence of Flower Micelles.** The analog of starlike micelles are flower micelles in the case of triblock copolymers. Their existence is still controversial from the theoretical and experimental point of view. Reference 24 concluded that they are forbidden for copolymer–homopolymer blends due to the backfolding energy. In the case of a selective solvent this penalty could be hidden by the effect of the osmotic pressure. This is investigated in the present section.

A spherical flower micelle made of $p$ triblocks molecules ($N_A$, $N_B$) is similar to a star micelle made of 2p diblocks ($N_A$, $N_B/2$) from the point of view of the blob scaling picture of the corona. As a consequence, the osmotic pressure term of the free energy is the same in both cases. Once again, there is a loss of entropy due to the backfolding of the middle B block. The polymer chains are stretched and thus the halves of the B block are close to each other. Using the Alexander–de Gennes approximation (all chains go the the edge of the corona[28]), the constraint is that the ends of the halves in neighboring blobs of the outer layer must meet. So, the loop penalty per chain can be shown to be $(3/2)\beta_{ev} \ln g(\xi_R)$, where the subscript ev stands for excluded volume and $g(\xi_R)$ is the number of monomers belonging to the largest blob. This is a straightforward application of eq 29 with $N = g(\zeta_R)$ and $r = \zeta_R$, so that the appropriate value for the coefficient $\beta$ is $\beta_{ev} \cong {}^6/_5$. Neglecting prefactors, the free energy per chain is

$$\frac{1}{p}F_{flower}/kT = \frac{1}{p}F_{star}(2p,N_A,N_B/2)/kT + \frac{3}{2}\beta_{ev}\ln\left(\frac{N_B}{\sqrt{p}}\right) \quad (35)$$

The last term does not really change the optimum aggregation number $p^*$ from that of a starlike micelle made of diblock copolymers but yields a shift in the chemical potential $\mu_{flower} = (1/p^*)F_{flower}(p^*)/kT$. Using numbers from solubility concentration measurements: $\gamma a^2 - (3(4\pi)^{1/2})^{2/3} \cong 0.2$, one obtains $p^* \cong 4$ and $\mu_{flower} \cong 14$. This value is due to a large looping shift on the order of 10. This result explains why flower micelles are not observed in our system since $\mu_{unimer} \cong 13$.

More generally, we now propose a kind of minimum stability criterion for a flower micelle by comparing it to the "stripped" flower obtained by pulling one A block out of the corona (Figure 15). The energy of this object is

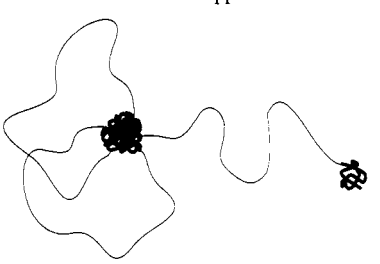


**Figure 15.** Flower-shaped conformation of triblock aggregates is unstable because of the loss of entropy due to the backfolding of the middle block. A stripped flower conformation, obtained by pulling one terminal block out of the corona, is more favorable.

$$F_{stripped}(p)/kT = F_{star}(2p-1,N_A,N_B/2)/kT + \frac{3}{2}(p-1)\beta_{ev}\ln\left(\frac{N_B}{\sqrt{p}}\right) + E_1/2kT \quad (36)$$

where $E_1/2$ corresponds to the energy of a free diblock ($N_A$, $N_B/2$). Setting $p = p^*$, one obtains

$$F_{flower}(p^*)/kT - F_{stripped}(p^*)/kT = \frac{1}{2}\left[\frac{1}{p^*}F_{flower}(p^*)/kT - E_1/kT + \frac{3}{2}\beta_{ev}\ln\left(\frac{N_B}{\sqrt{p^*}}\right)\right] \quad (37)$$

As a result, if

$$\frac{N_B}{\sqrt{p^*}} \geq \left(\frac{1}{\phi_{c.m.c.}}\right)^{2/3\beta} \quad (38)$$

the flower conformation is certainly unstable, where $\phi_{c.m.c.}$ is the critical micellar concentration for flowers to appear.

For the PS–PI–PS copolymer we have dealt with, we can estimate the free energy gain on extruding one block to be about 6 $kT$ and several arms must be pulled out for a substantial energy gain. Obviously micelles made of triblocks having free terminal blocks tend to associate and yield extended structures (see section 4.2.4).

**4.2.3. Other Compact Aggregates: Tubes, Platelets, etc.** The study of spherical micelles has shown that the loop entropy is related to the size $\zeta_R$ of the outer blobs. Because of the radial structure $\zeta_R$ is rather large. It is worth comparing with, e.g., cylindrical or lamellar (platelets...) aggregates for which $\zeta_R$ is smaller. The loop energy per chain is found to be[29]

cylinder
$$F_{loop}/kT = \frac{3}{2}\beta_{ev}\frac{5}{8}\ln\left(\frac{\lambda}{a}N_B\right) \quad (39)$$

lamella
$$F_{loop}/kT = \frac{3}{2}\beta_{ev}\frac{5}{6}\ln\left(\frac{\Sigma}{a^2}\right) \quad (40)$$

where $\lambda$ and $\Sigma$ are the cylinder length and the lamella area per chain, respectively. Numerically we get $\mu_{cyl} \cong 13$, slightly less than $\mu_{flower}$, while $\mu_{lam}$ is much higher. Although improbable in our case, the possible existence of cylinders (in particular for the longer B block) should be kept in mind.

**4.2.4. Loose Aggregates.** The above considerations show how entropic effects due to the middle block backfolding prevent the existence of classical micelles. Thus we expect aggregates with several A cores, very few loops and thus rather loose and extended conformation. This is confirmed experimentally. A more precise description of these objects is difficult. Branched or treelike structures can be considered. The experimental situation is probably complicated by the polydispersity of aggregates (small $p$), as it is confirmed by the unimer concentration

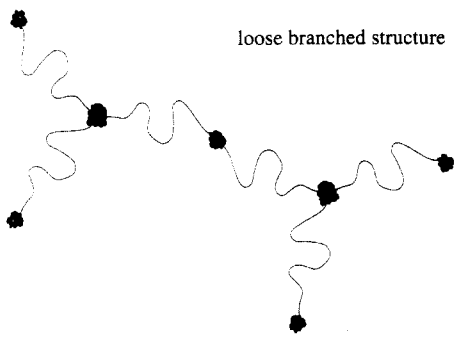


**Figure 16.** Possible loose structure for triblock aggregates.

which increases with the total concentration above the *c.a.c.* (see section 4.1 and Figure 12).

Assuming an infinite branched structure with mean functionality $f$, the observed value of $\phi_{c.a.c.}$ gives the estimate $f \cong 6$ from:

$$2f^{-1/3}\gamma a^2(3(4\pi)^{1/2}N_A)^{2/3} = E_1 + \ln \phi_{c.a.c.} \quad (41)$$

if excluded-volume effects are neglected. These latter effects should yield to clusters of finite size. In view of the high values of the apparent radius of the aggregates, $R_{app}$, reported here, it is tempting to propose a linear structure ($f = 2$). But, this would correspond to an energy per chain $\mu_{lin} \cong 10$ (taking into account surface tension only), and a critical concentration $\phi_{c.a.c.} \cong 5 \times 10^{-2}$ g/g. Moreover, excluded-volume effects strongly limit the length of such a chain.

The measured value of $R_{app}$ is much too large to be that of a typical aggregate. As discussed in section 4.1, $R_{app}$ corresponds to the radius of the largest objects and the fact that it does not scale as $p^{1/d_f}$ was ascribed to the polydispersity. However, the existence of a rather sharp *c.a.c.* suggests that there is some optimal aggregation number different from unity giving a sizable decrease of the chain chemical potential. The largest aggregates could be the result of stripped flowers "holding hands" in chain (Figure 16). Within such a picture each isolated stripped flower looks like a star having such a small number of polyisoprene arms that the latter would have no more than one or two blobs. As a matter of fact, the radius of the polystyrene cores can be estimated to be on the order of 40 Å (assuming Gaussian conformation of the chain and from ref 30); this leads to a smallest blob having a size $\zeta \cong 60$ Å, while a homopolyisoprene having the same mass as the middle block of our sample is expected to have a radius equal to 150 Å.[31] The first consequence of these estimates is that this structure is compatible with the observation of internal modes. The second consequence is that the overlap concentration of the aggregates, i.e., their internal concentration, would be the one of unimers: $1.7 \times 10^{-2}$ g/cm$^3$, in agreement with viscosity measurements.

## 5. Conclusion

In this paper we have reported static and dynamic light scattering experiments performed on triblock copolymers in dilute solution in a selective solvent. The results do not correspond to those expected for a micellar structure of the aggregates but rather are consistent with a loose branched structure: (1) the form factor of the aggregates shows a smooth decrease at $qR > 1$; (2) quasi-elastic light scattering data indicate internal modes; (3) viscosity measurements show that the internal concentrations of unimers and aggregates are identical; (4) the unimer concentration and the aggregation number depend on the copolymer concentration. To our knowledge, this is in contradiction to most of the experimental results reported in the literature. Simple theoretical considerations have shown that this result is understandable, taking into account the entropic term corresponding to the backfolding of the middle block. This term depends strongly on the size of the two terminal blocks and on the interfacial tension between these blocks and the solvent. These are the relevant parameters that have to be controlled in order to observe a transition from loose to micellar structures. Nevertheless, this work outlines the major difference between diblock and triblock behaviors. Further experiments have to be performed in this direction.

Light and neutron scattering experiments and rheological measurements were performed in semidilute solution on the same triblock/solvent system. These results will be reported in a following paper.

**Acknowledgment.** We thank P. Pincus for enriching discussions as well as A. Halperin and M. Tirrell for stimulating comments.

## References and Notes

(1) Chu, B. *Laser Light Scattering*, 2nd ed.; Academic Press, Inc.: San Diego, CA, 1991; p 290.
(2) Tuzar, Z.; Kratochvil, P. *Surf. Colloid Sci.* **1992**, *15*, 1.
(3) Berne, B. J.; Pecora, R. *Dynamic Light Scattering*; John Wiley: New York, 1976.
(4) de Gennes, P.-G. *Scaling Concepts in Polymer Physics*; Cornell University Press: Ithaca, NY, 1979.
(5) Adam, M.; Delsanti, M. *J. Phys. Lett.* **1977**, *38*, L-271.
(6) Witten, T. A.; Pincus, P. A.; Cates, M. E. *Europhys. Lett.* **1986**, *2*, 137.
(7) Adam, M.; Fetters, L. J.; Graessley, W. W.; Witten, T. A. *Macromolecules* **1991**, *24*, 2434.
(8) Dubois-Violette, E.; de Gennes, P.-G. *Physics* **1967**, *3*, 181.
(9) Langowski, J.; Bryan, R. *Macromolecules* **1991**, *24*, 6346.
(10) Perzynski, R. Ph.D. Thesis, Université Pierre et Marie Curie, France, 1984.
(11) Leibler, L.; Orland, H.; Wheeler, J. C. *J. Chem. Phys.* **1983**, *79*, 3550.
(12) Halperin, A. *Macromolecules* **1989**, *22*, 3806.
(13) Halperin, A.; Tirrell, M.; Lodge, T. P. *Adv. Polym. Sci.* **1992**, *100*, 31.
(14) Plestil, J.; Baldrian, J. *Makromol. Chem.* **1975**, *176*, 1009.
(15) Hilfiker, R.; Chu, B.; Xu, Z. *J. Colloid Interface Sci.* **1989**, *133*, 176.
(16) Halperin, A. *Macromolecules* **1991**, *24*, 1418.
(17) Balsara, N. P.; Tirrell, M.; Lodge, T. P. *Macromolecules* **1991**, *24*, 1975.
(18) Plestil, J.; Hlavata, D.; Hrouz, J.; Tuzar, Z. *Polymer* **1990**, *31*, 2112.
(19) Tuzar, Z.; Konak, C.; Plestil, J.; Kratochvil, P.; Prochazka, K. *Polymer* **1990**, *31*, 2118.
(20) Richter, D.; Farago, B.; Fetters, L.; Huang, J. S.; Ewen, B. *Macromolecules* **1990**, *23*, 1845.
(21) Adam, M.; Lairez, D. *Fractals* **1993**, *1*, 149.
(22) Munch, J. P.; Delsanti, M.; Adam, M., unpublished results.
(23) Corona-Vallet, S.; Lairez, M.; Adam, M.; Carton, J. P., to be published.
(24) ten Brinke, G.; Hadziioannou, G. *Macromolecules* **1987**, *20*, 486.
(25) Wang, Y.; Mattice, W. L.; Napper, D. H. *Macromolecules* **1992**, *25*, 4073.
(26) des Cloizeaux, J. *Phys. Rev. A* **1974**, *10*, 1665.
(27) Zimm, B. H.; Stockmayer, W. H. *J. Chem. Phys.* **1949**, *17*, 1301.
(28) Alexander, S. *J. Phys. (Paris)* **1977**, *36*, 98. de Gennes, P.-G. *Macromolecules* **1980**, *13*, 1069.
(29) Wang, Z.-G.; Safran, S. A. *J. Chem. Phys.* **1989**, *88*, 5328.
(30) Schmidt, M.; Burchard, W. *Macromolecules* **1981**, *14*, 210.
(31) Davidson, N. S.; Fetters, L. J.; Funk, W. G.; Hadjichristidis, N.; Graessley, W. W. *Macromolecules* **1987**, *20*, 2614.